

## Article

# *Djck1 $\alpha$* Is Required for Proper Regeneration and Maintenance of the Medial Tissues in Planarians

Yongding Huang<sup>1</sup>, Yujia Sun<sup>1</sup>, Yajun Guo<sup>1</sup>, Mengwen Ma<sup>1</sup>, Shoutao Zhang<sup>1,2,\*</sup> and Qingnan Tian<sup>1,\*</sup> <sup>1</sup> School of Life Sciences, Zhengzhou University, Zhengzhou 450001, China<sup>2</sup> Longhu Laboratory of Advanced Immunology, Zhengzhou 450000, China

\* Correspondence: zhangst@zzu.edu.cn (S.Z.); tianqn@zzu.edu.cn (Q.T.)

**Abstract:** CK1 $\alpha$  (Casein kinase 1 $\alpha$ ) is a member of the casein kinase 1 (CK1) family that is involved in diverse cellular processes, but its functions remain unclear in stem cell development. Freshwater planarians are capable of whole-body regeneration, making it a classic model for the study of regeneration, tissue homeostasis, and polarity in vivo. To investigate the roles of CK1 $\alpha$  in regeneration and homeostasis progress, we characterize a homolog of CK1 $\alpha$  from planarian *Dugesia japonica*. We find that *Djck1 $\alpha$* , which shows an enriched expression pattern in the nascent tissues, is widely expressed especially in the medial regions of planarians. Knockdown of CK1 $\alpha$  by RNAi presents a thicker body due to dorsal hyperplasia, along with defects in the medial tissues including nerve proliferation, missing epidermis, intestine disturbance, and hyper-proliferation during the progression of regeneration and homeostasis. Moreover, we find that the *ck1 $\alpha$*  RNAi animals exhibit expansion of the midline marker *slit*. The eye deficiency induced by *slit* RNAi can be rescued by *ck1 $\alpha$*  and *slit* double RNAi. These results suggest that *ck1 $\alpha$*  is required for the medial tissue regeneration and maintenance in planarian *Dugesia japonica* by regulating the expression of *slit*, which helps to further investigate the regulation of planarian mediolateral axis.

**Keywords:** *Djck1 $\alpha$* ; *Djslit*; mediolateral axis; stem cells; regeneration; planarian



**Citation:** Huang, Y.; Sun, Y.; Guo, Y.; Ma, M.; Zhang, S.; Tian, Q. *Djck1 $\alpha$*  Is Required for Proper Regeneration and Maintenance of the Medial Tissues in Planarians. *Cells* **2023**, *12*, 473. <https://doi.org/10.3390/cells12030473>

Academic Editor: Christian Dani

Received: 12 October 2022

Revised: 15 January 2023

Accepted: 30 January 2023

Published: 1 February 2023



**Copyright:** © 2023 by the authors. Licensee MDPI, Basel, Switzerland. This article is an open access article distributed under the terms and conditions of the Creative Commons Attribution (CC BY) license (<https://creativecommons.org/licenses/by/4.0/>).

## 1. Introduction

Substrate phosphorylation, mediated by protein kinases, is a common modification that plays an essential role in the regulation of various cellular functions [1,2]. The casein kinase 1 (CK1) family is a group of evolutionarily conserved monomeric serine (Ser)/threonine (Thr) protein kinases found in eukaryote organisms ranging from yeast, plants, algae, and protozoa to mammals [3–7]. CK1 participates in numerous developmental signaling including the Hedgehog (Hh) and Wnt signaling pathways [8,9]. It has been implicated in a variety of cellular functions, including DNA processing and repair, cell division, cytoskeleton dynamics, membrane receptor trafficking, circadian rhythms, and cell differentiation [10–13]. Seven isoforms from the CK1 family are found in mammals ( $\alpha$ ,  $\beta$ ,  $\gamma$ 1,  $\gamma$ 2,  $\gamma$ 3,  $\delta$ , and  $\epsilon$ ), whereas eight are found in *Drosophila*, and 87 members are found in *C. elegans* [14–16]. All members have a highly conserved kinase domain in mammals [17]. Among them, Casein kinase 1 $\alpha$  (CK1 $\alpha$ ) has been confirmed to be crucial for the phosphorylation of  $\beta$ -catenin at the destruction complex (a known major component of the Wnt pathway) [4,18,19]. However, the function of CK1 $\alpha$  in stem cells was not yet defined. Data from several previous studies suggest that CK1 $\alpha$  participates in polarity development, especially the regulation of axial polarity whereas understanding its regulation remains challenging [20–22].

Planarian is a member of the phylum Platyhelminthes with an almost unparalleled ability to regenerate the missing tissues and rebuild the whole body after being injured. It is considered to be an outstanding model for studying regeneration and polarity reconstruction [23–26]. As constitutive flat animals, planarians have sophisticated anatomy,

including the brain, eyes, intestine, musculature, and epidermis, all arranged in complex and appropriate patterns [27,28]. It can regenerate a complete individual from almost any irregularly shaped fragment, owing to an abundant adult somatic stem cell population (called neoblasts, approximately ten percent of all animal cells) [25,29–32]. Furthermore, a process known as tissue turnover means that the neoblasts of adult planarians constantly produce new cells to replenish dying ones, demonstrating the remarkable capability to regenerate in planarians [25]. The tissue turnover and regeneration process require the new cells to differentiate and to form in the location in the body correctly, for example, new tail cells need to form in the posterior pole, and new eye cells need to form in the heads [33]. Position control genes (PCGs), some of which are involved in tissue regeneration and polarity reconstruction, are required for the orderly expression of several genes throughout the dynamic and complicated tissue turnover and regeneration process [34–36]. PCGs control tissue identity along the anterior–posterior (AP) axis, the dorsal–ventral (DV) axis, and the medial–lateral (ML) axis in planarians. For example, a canonical  $\beta$ -catenin-dependent Wnt signaling pathway is required for anteroposterior blastema polarity in planarian regeneration [37–39]. Upregulation of the canonical Wnt negative regulators *notum* and *APC* causes the regeneration of ectopic tails whereas downregulation of Wnt pathway components  *$\beta$ -catenin-1*, *Evi/wntless*, *wnt1*, *Dvl-1/2* or *teashirt* causes the ectopic heads [40–44]. The bone morphogenetic protein (BMP) pathway has been shown to play an important role in the dorsoventral axis. After BMP pathway silencing, the DV axis in planarians is disrupted [45,46]. The planarian midline is regulated by *slit*, which acts as a repulsive cue required for proper midline formation. The suppression of *slit* can cause the medial tissue defects and a collapse of regenerating central nervous system (CNS) [47]. It is now well established that planarian presents a robust system for studying polarity; however, the mechanisms of controlling positional information have remained unclear.

In our work, we characterize a homolog of CK1 $\alpha$ , a member of the casein kinase 1 family, from planarian *Dugesia japonica*. We show that RNA interference targeting *ck1 $\alpha$*  causes a wide range of regeneration and tissue homeostasis defects such as intestine disorder, epidermis absence, and neurologic abnormality in medial tissues. Meanwhile, the division of phospho-H3 mitotic cells is increased in both regenerating and intact *ck1 $\alpha$*  RNAi planarians. CK1 $\alpha$  RNAi in planarians revealed some phenotypes that were opposite to the *slit* RNAi phenotypes. We propose that *ck1 $\alpha$* , which regulates the expression levels of the *slit*, is required for the regeneration and maintenance of medial tissues in planarians.

## 2. Materials and Methods

### 2.1. Planarian Culture

An asexual strain of planarian *Dugesia japonica* was cultured in autoclaved stream water at 22 °C, as previously described [48,49]. Planarians 5–9 mm in length were selected and starved for at least 7 days before the experiments.

### 2.2. Gene Identification and Cloning

Ck1 $\alpha$  sequences from planarian *Dugesia japonica* species were identified in the planarian transcriptome [50]. A pair of specific primers (*Djck1 $\alpha$ F* and *Djck1 $\alpha$ R*) were designed to amplify the *Djck1 $\alpha$*  from cDNA (extracted from intact planarians). The *Djck1 $\alpha$*  sequence was cloned into PMD-19-Vector (Takara, Kyoto, Japan) for further experiments. All primers used for *Djck1 $\alpha$*  and *Djslit* cloning and dsRNA generation are listed in Table S1.

### 2.3. RNAi Experiments

The double-stranded RNAs of *Djck1 $\alpha$*  were synthesized by in vitro transcription as previously described [49,51]. The dsRNA was dissolved in RNase-free H<sub>2</sub>O (water treated by DEPC). The *Djck1 $\alpha$*  dsRNA was injected into the experimental planarians using a Drummond microinjector, while the control animals were injected with water treated by DEPC. The dsRNA concentration used for injection was 2  $\mu$ g/ $\mu$ L. The volume of dsRNA was 0.8  $\mu$ L, once per planaria. The injection site was mainly on the dorsal side, which varied day to

day, and the injection rate was once each day. Animals were injected consistently for a week, unless otherwise stated, and heads and tails were amputated 24 h after the last injection.

#### 2.4. Whole-Mount Immunostaining

Whole-mount immunostaining was performed as previously described [52]. In brief, the animals were killed with 5% NAC in phosphate-buffered saline (PBS) for 6 min at room temperature and washed four times with PBS containing 0.1% TritonX-100 (PBST). Then, the animals were fixed in PBST containing 4% paraformaldehyde. Next, the animals were blocked with 10% goat serum in PBST for 2 to 4 h at 4 °C and incubated with primary anti-H3P (1:500; Millipore, Burlington, MA, USA, 05-817R) or anti-synapsin (1:100–1:500 Developmental Studies Hybridoma Bank) antibodies overnight. The secondary antibodies include goat anti-rabbit Alexa Fluor 568 (1:500; Invitrogen, Waltham, MA, USA, 11036) for anti-H3P, and goat anti-mouse Alexa Fluor 488 (1:500; Invitrogen, 673781) for anti-synapsin. Digital pictures were collected using NIS element software (version 4.2.0, Nikon, Tokyo, Japan).

#### 2.5. In Situ Hybridization

As previously described, Whole-mount in situ hybridizations (WISHs) were performed with digoxigenin-labeled probes [53]. All samples were hybridized with a DIG-labeled probe at 56 °C for at least 16 h. Colorimetry (NBT/BCIP) was subsequently used to detect the signal.

#### 2.6. Quantitative RT-qPCR

Total RNA was extracted using Trizol reagent (TaKaRa, Gunma, Japan), and cDNA was synthesized from 1 µg of total RNA with oligo-dT primers and reverse transcriptase based on the manufacturer's protocol (TaKaRa). Quantitative real-time PCR was performed as previously described [53]. Three replicates were run in parallel for each condition. Data were normalized to expression level elongation factor 2 (*Djef2*) [54]. The  $2^{-\Delta\Delta CT}$  method, which was described by Schmittgen and Livak, was used to calculate expression ratios [55]. The primers used for quantitative real-time PCR are listed in Supplementary Table S1.

#### 2.7. Statistical Analysis

The data for gene expression are presented as means  $\pm$  SD (mean and standard deviation). Statistical analyses were performed using unpaired Student's *t*-test. One-way analysis of variance was used for analyzing two or more groups of data. Differences were considered significant at  $p < 0.05$  level and extremely significant at  $p < 0.01$  level.

### 3. Results

#### 3.1. *Djck1α* Expresses in the Middle and Is Required for Normal Tissue Regeneration and Maintenance

To better investigate the role of CK1 $\alpha$  in planarian regeneration, we identified a *ck1α* homolog in *Dugesia japonica* (*Djck1α*) and the full-length cDNA of *Djck1α* was obtained by PCR based on the transcriptome (Figure S1) [50]. Then, we performed whole-mount in situ hybridization in regenerative and intact animals to investigate spatiotemporal expression patterns. The animals were amputated before and after the pharynx into three sections: head, trunk, and tail, for regenerating, and were fixed at 1, 3, 5, and 7 days after amputation. The WISH results revealed that the expression of *Djck1α* was detected throughout the body except the pharynx in intact animals, with positive signals found clearly in the midline (Figure 1A). In regenerating animals, a higher expression level of *Djck1α* was detected in the wound region after amputation, and this pattern of expression persisted throughout the regeneration process. By 7 days post amputation, the newly regenerated heads and tails were completed, and *Djck1α* was mainly distributed in the new body parts.

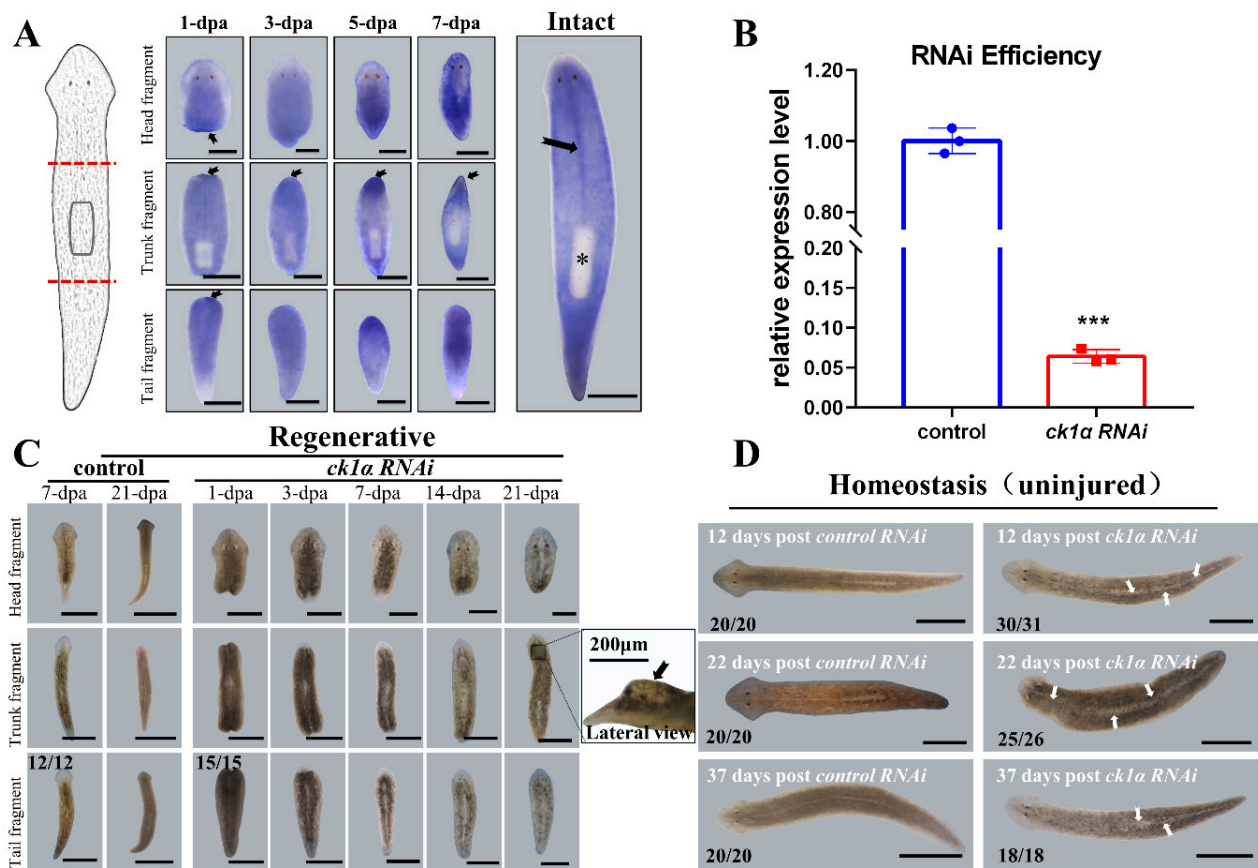


**Figure 1.** Spatiotemporal expression patterns and RNAi defects of *ck1α* in planarians. (A) Spatiotemporal expression patterns of *ck1α* in *Dugesia japonica*. Amputation sites indicated by red dotted lines on the left. Higher expression in the wound regions and the middle, indicated by black arrows. (dpa, days post amputation;  $n = 6$  per condition. \* pharynx without positive signaling.) (B) QRT-PCR for the downregulation efficiency of *ck1α* RNAi at 48 h after the last injection. Unpaired Student's *t*-test, Mean  $\pm$  SD. \*\*\*  $p < 0.001$ . Six planarians per group and three replicates per condition. (C) Regeneration defects induced by injecting *ck1α* dsRNA into planarians. Animals were amputated pre- and post-pharyngeally after the last injection. Dorsalis protuberances (dotted box and black arrow) in 21 dpa trunks. (D) Live images of homeostatic *ck1α* RNAi animals at different times post the last injection. White arrows: visible 'white lines' in the middle. Scale bars: 500  $\mu$ m.

The endogenous *Djck1α* was knocked down by RNAi, and the downregulation efficiency was demonstrated using qRT-PCR (Figure 1B). The RNAi planarians' regeneration rate was perceived to be slower than that of the controls during regenerating (29/29). The *Djck1α* RNAi planarians were unable to regenerate heads and tails that were the proper size and form. The new heads lacked a clear 'triangular structure', and the new tails were shorter (Figure 1C). Dramatically, there was the probability of observing a 'protruding outgrowth' in the 21 days regenerative animals below the newly generated head on the dorsal side (8/21) (Figure 1C). In intact animals, there was no obvious difference in appearance in the first week after RNAi; however, a visible 'white line' was observed on the dorsal side in the middle of the body starting from the tail at about 14 days after RNAi. As RNAi proceeded, the 'white line', which is clearly visible as an 'outgrowth line' on the dorsal side, lengthened and became more apparent from the tail to the head (Figure 1D). It is possible that *Djck1α* plays a substantial role in the regeneration and maintenance of medial tissues based on the unique yet robust expression of *ck1α* and the phenotype induced by silencing *Djck1α* in intact and regenerated animals.

### 3.2. *Djck1α* Inhibition Causes Abnormalities in Nervous, Intestine, and Epidermis Systems during Regeneration

Since the RNAi of *Djck1α* resulted in the formation of smaller heads and tails with evident outgrowth on their dorsal side, we performed the WISH with *Djpc-2* and the whole mount immunofluorescence for anti-synapsin (Syn) to determine the development of the nervous systems [56–59].

The RNAi phenotypes observed in head and tail fragments could be detected in the trunk fragments simultaneously. Therefore, except as otherwise noted, the subsequent studies were mainly conducted using the trunks. The results showed that the complete and closed ventral nervous cords (VNCs) existed in the *Djck1α* RNAi animals after 10 days of regeneration, whereas both the width of the VNCs and the distance between two ventral nerve cords increased (Figure 2A). Additionally, we detected that *Djck1α* RNAi animals exhibited more diffuse staining of the cephalic ganglion areas with unclear boundaries in all cases (100%) (Figure 2A).

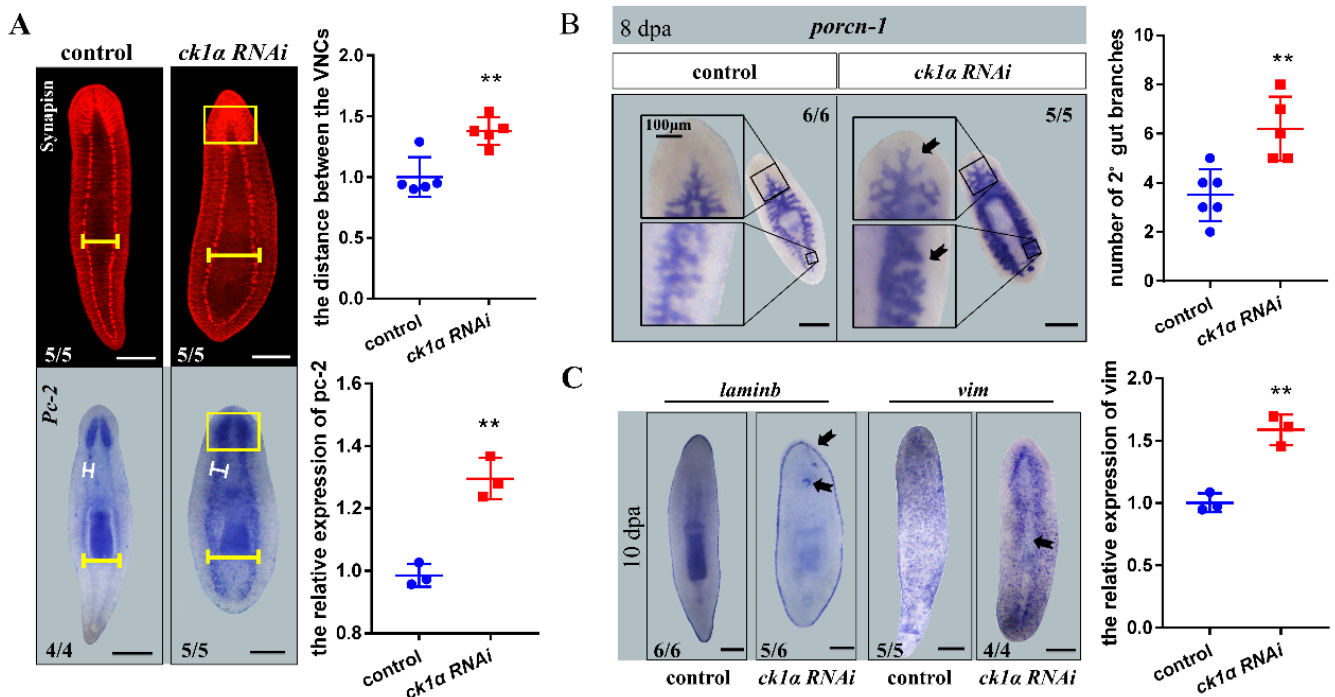


**Figure 2.** *Djck1α* RNAi animals show drastic differences in the growth of nervous, intestine, and epidermis systems. (A) Nervous systems in trunk fragments 15 dpa. Anti-synapsin and *pc-2* riboprobe. *Ck1α* RNAi trunk fragments exhibited blurry cephalic ganglia (Yellow boxes), wider ventral nervous cords (white bar), and a longer distance between them (yellow bar). Upper right: the distance of the VNCs. Bottom right: Quantification of *pc-2*. Unpaired Student’s *t*-test, Mean ± SD. \*\* *p* < 0.01. (B) Intestinal defects (black arrows) in *ck1α* RNAi animals. Stronger expression and more branches of intestines on the right (black boxes). Right: The number of secondary gut branches. Mean ± SD. Unpaired Student’s *t*-test. (C) Abnormal expression patterns in trunk fragments (black arrows) of epidermis marker genes (*laminb*, *vim*) by FISH. Right: Quantification of *vim*. Unpaired Student’s *t*-test, Mean ± SD. \*\* *p* < 0.01. Scale bars: 300 μm.

By day 8, when the control animals had regenerated completely, the *Djck1α* RNAi animals were observed to lose the ingestion behavior. Therefore, we performed whole-mount in situ hybridization to identify the variation of the gut by using probes for *Djporcn-1* [44]. The gut of the control animals consisted of a single branch anteriorly, which bifurcates into two detached posterior branches at the pharynx (Figure 2B). However, in *Djck1α* RNAi animals, intestinal morphology showed more robust expression, and more secondary and tertiary branches throughout the intestinal system (Figure 2B).

To investigate the ‘middle line’ on the dorsal of the intact *Djck1 $\alpha$*  RNAi animals, we then performed WISH with *Djvim* (the differentiated mature epidermal cells marker) and *Djlamini* (the epidermal boundary marker) 10 days after RNAi [60–63]. Considering the previously observed phenotypes, the planarian epidermis was possibly separated by the ‘medial line’; in the meantime, the WISH results suggested the same possibility. Compared to the control animals, which possess the intact epidermis, the expression of *Djvim* in the *Djck1 $\alpha$*  RNAi animals showed conspicuous missing at the ‘medial line’ region (Figure 2C). The expression patterns of *Djlamini* were consistent with the controls overall; however, some animals (7/12) showed positive signal out of border position (Figure 2C). The WISH results of *Djmhc-a* (a marker of the pharynx in *Dugesia japonica*) showed that *Djck1 $\alpha$*  RNAi had no significant effect on pharynx regeneration (Figure S2) [64].

Taken together, these findings provide important evidence for the variation of the medial tissues, suggesting that the cell proliferation and fate determination probably differ caused by the knockdown of *Djck1 $\alpha$* .

### 3.3. *Djck1 $\alpha$* RNAi Results in Hyper-Proliferation

As stated previously, the constitutive animals, *Dugesia japonica*, possess a highly active pool of adult somatic stem cells called neoblasts, some of which are pluripotent and serve as the cellular basis for regeneration. Cell proliferation and differentiation requires the appropriate choices of fate. Inapposite fates can result in hyper- or hypo-proliferative pathological states [65]. Since CK1 $\alpha$  plays a vital role in cell division, the unique phenotype of *Djck1 $\alpha$*  RNAi animals may indicate the effect on cell proliferation. Whole-mount immunofluorescence for phosphorylated histone H3 (Phospho-H3 which marks cells during the G2/M transition of the cell cycle) was performed to investigate how *Djck1 $\alpha$*  RNAi affects cell proliferation. Probes for *Djpiwi-1* (a molecular probe labeled with undifferentiated neoblasts) were used to analyze the effect of *Djck1 $\alpha$*  RNAi on neoblasts [66,67].

We counted the number of phosphorylated H3 cells in the head, trunk, and tail fragments, respectively, at 3 days after amputation, but found no significant difference between *Djck1 $\alpha$*  RNAi animals and the controls (Figure 3A). However, by day 8, in regenerating animals, a positive increase in the number of phosphorylated H3 cells was observed in *Djck1 $\alpha$*  RNAi animals compared to the controls, especially in the region where outgrowth may subsequently arise (Figure 3A). Meanwhile, increased expression of *Djpiwi-1* was detected in the particular region backing onto the newly regenerative heads and tails (Figure 3A), suggesting that downregulation of *ck1 $\alpha$*  may increase cell proliferation in particular organizations.

In intact *Djck1 $\alpha$*  RNAi animals, we also found that the number of phosphorylated H3 cells increased at 8 days, which was consistent with the results in regenerating *Djck1 $\alpha$*  RNAi animals. Meanwhile, the WISH results of *Djpiwi-1* presented the same upward trend. Similar results were obtained by analyzing the expression levels of the same markers by qRT-PCR. These were highly expressed in intact *Djck1 $\alpha$*  RNAi animals from medial to lateral (Figure 3B); furthermore, the region with higher expression levels of *Djpiwi-1* usually occupied the same position as the area in which enation appeared (Figure 3B,C). Overall, these results indicate that the downregulation of *Djck1 $\alpha$*  can cause hyper-proliferation in both the tissue turnover and regeneration processes.

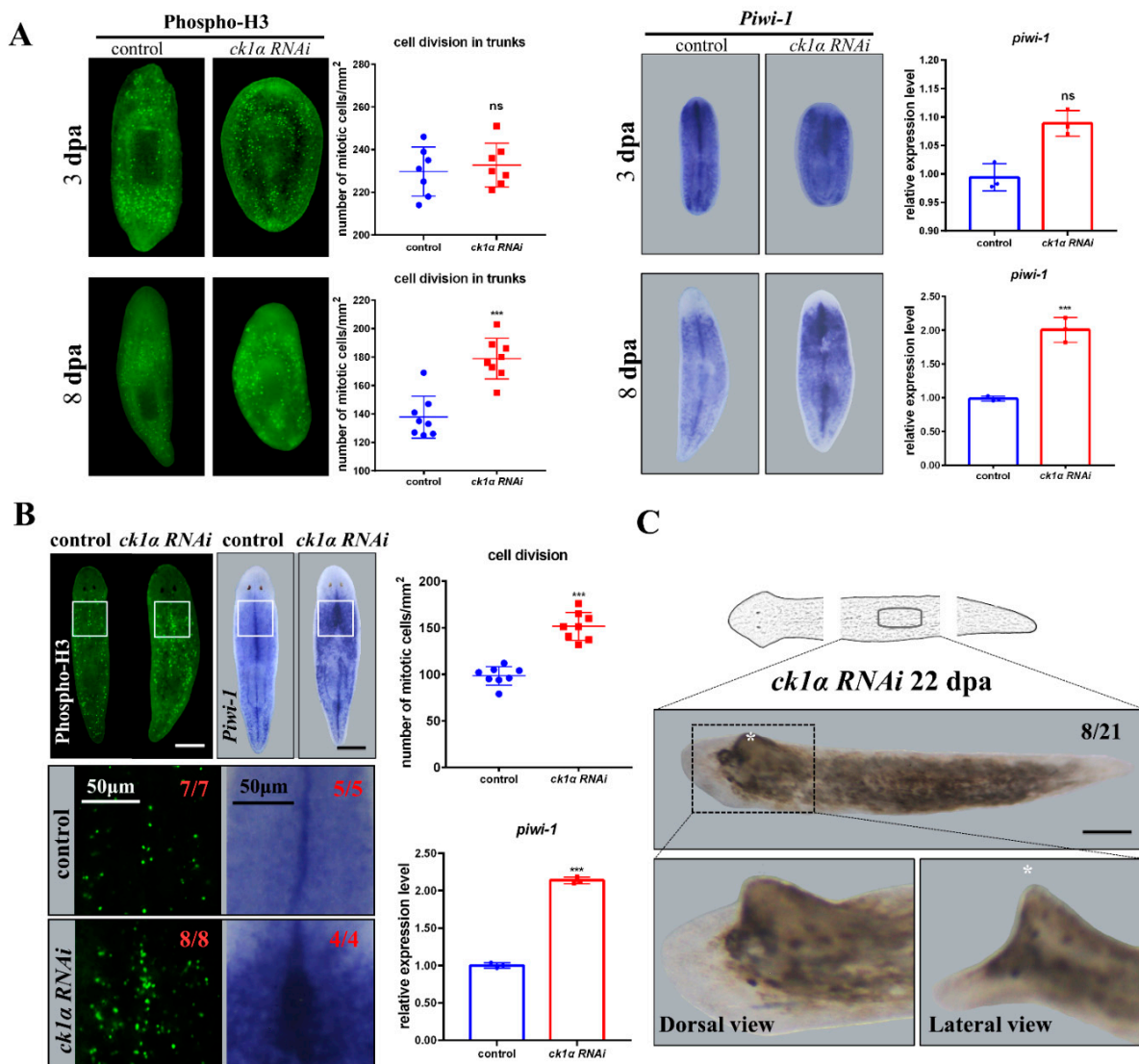


**Figure 3.** Knockdown of *Djck1α* promotes cell proliferation in both regenerative and intact planarians. (A) Phospho-H3 IF and *piwi-1* WISH were performed to detect cell proliferation. RNAi animals were fixed at indicated time points. Left: Quantitative statistical analysis for Phospho-H3 cells. Right: Quantification of *piwi-1*. Unpaired Student's *t*-test, Mean ± SD. ns  $p > 0.05$ . \*\*\*  $p < 0.001$ . (B) Generation of undifferentiated cells was examined by Phospho-H3 IF and *piwi-1* WISH in intact RNAi animals. Intact RNAi animals were fixed at 8 dpi (days post last injection). The positive cells were quantified in the dorsal region (white boxes). Upper right: Quantitative statistical analysis for Phospho-H3 cells. Bottom right: Quantification of *piwi-1*. Unpaired Student's *t*-test, Mean ± SD. ns  $p > 0.05$ . \*\*\*  $p < 0.001$ . (C) Regenerating RNAi trunk fragments at 22 dpa. \* Outgrowth on the dorsal region. Scale bars: 300 μm.

### 3.4. Inhibition of *Djck1α* Affects Tissue Turnover and Generates Medial Tissue Dilation in Intact Planarians

We had shown the hyper-proliferation defects in medial tissue were induced by the *Djck1α* RNAi during regenerating progress. To further explore the role of *Djck1α* in the maintenance of medial tissues in homeostasis, we next detected the nervous, intestine, and epidermis systems in the intact (uninjured) *Djck1α* RNAi animals.

The VNCs showed the same variation as previously described, including the wider distance between two nervous cords and stronger expression of the whole nervous system, especially in the cephalic ganglia (CG), which could be a kind of consequence of cell

overproliferation (Figure 4A). Meanwhile, we observed drastic changes in gut morphology in intact planarians, including the exceptional connection at two parallel posterior branches in the middle (5/7), more secondary branches, and increased diffuse background before the pharynx (7/7) (Figure 4B). The *Djvim* WISH results showed that missing epidermis in the middle were timed to coincide to the ‘white line’ phenotype in Figure 1D, evolving most noticeably by day 39 (Figure 4C).

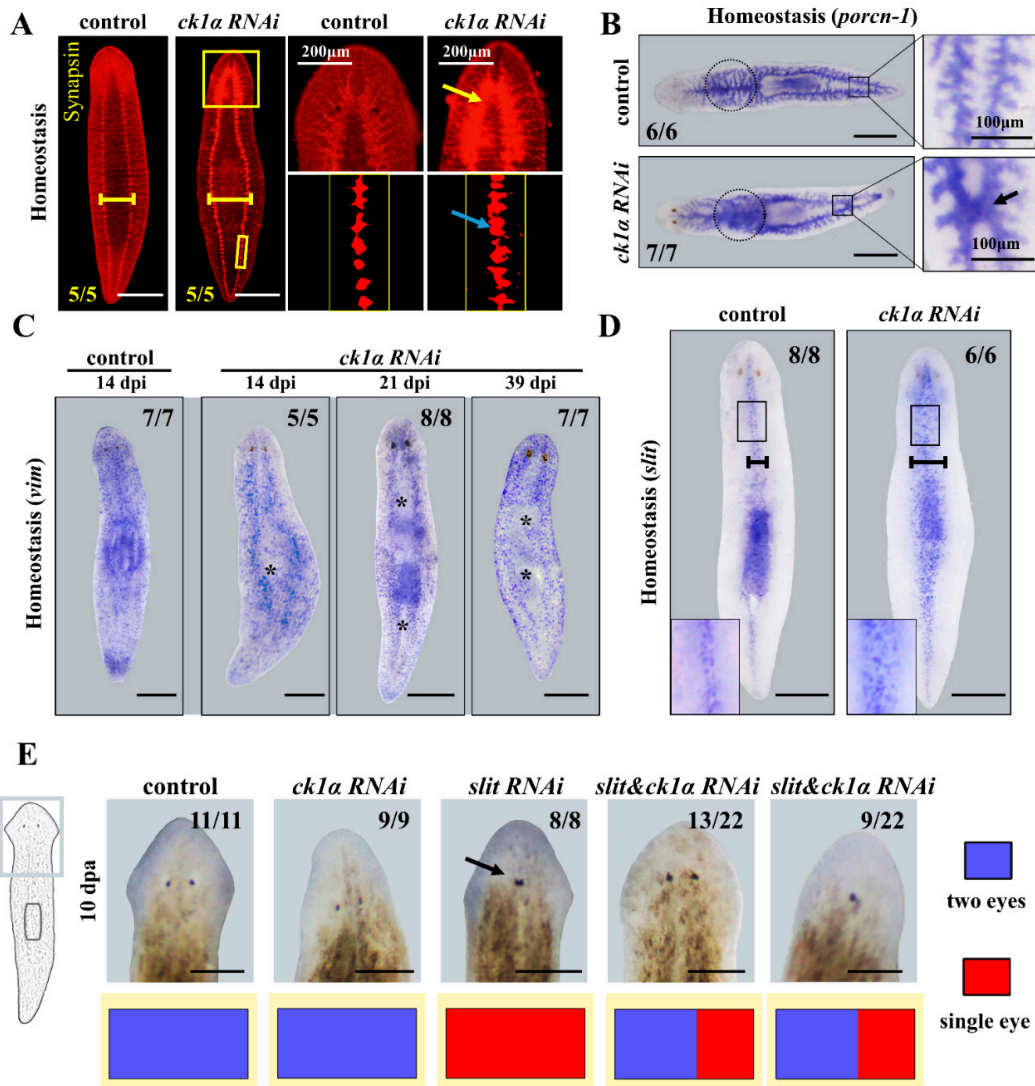


**Figure 4.** Influence of *Djck1α* RNAi on nerves, intestines, epidermis, and medial tissues in intact planarians. (A) Control and *ck1α* RNAi intact planarians at 20 dpi, stained with anti-Synapsin. Yellow arrows point to CG, blue arrows to VNCs. Note the expression and expansion of nervous tissue in *ck1α* RNAi animals (yellow boxes). Yellow bar: distance between VNCs. (B) Whole-mount in situ hybridization analysis of *Djporcn-1* mRNA in intact animals. Black arrows indicate the connection in the middle between two posterior branches of the gut. Increased diffuse background was perceived before the pharynx (Black dotted circles). (C) Whole-mount in situ hybridization of *vim* as an epidermis marker in intact animals at indicated time points. \* Absence of epidermis in the middle of the body. (D) Expansion of the midline in intact planarian at 20 dpi. Middle line: *slit* riboprobe. Black bar: the extent of *slit* expression. (E) Eye number statistic in regenerating heads after RNAi. Black arrow: single eye in regenerative heads of *slit* RNAi animals. Scale bars: 400 µm; except E, 200 µm.

The correct and ordered differentiation of neoblasts is essential for the maturation and maintenance of the planarians. The outgrowth in intact animals on the dorsal side had

not yet developed into the epidermis (Figure 4C). In consideration of the distinct middle expression of *Djck1 $\alpha$*  and the medial outgrowth phenotypes obtained from *Djck1 $\alpha$*  RNAi animals, we speculated that there was likely a kind of relationship between *ck1 $\alpha$*  and *slit* (a marker of the planarian midline).

We first analyzed the expression of *Djslit*, which is expressed in a medial domain, as previously reported (Figure 4D) [47]. Next, we detected the discrepancy of expression of *Djslit* in intact *Djck1 $\alpha$*  RNAi animals. As predicted, 100% of *Djck1 $\alpha$*  RNAi animals showed increased expression of *Djslit*, which was denser and expanded in the medial tissues (Figure 4D). Taken together, these results suggested that CK1 $\alpha$  can restrict the expansion of the medial tissues, including *slit* expressing cells. For the knockdown of *Djck1 $\alpha$*  caused overexpression of *Djslit*, we next assayed whether the *Djslit* RNAi phenotypes can be rescued by double-RNAi experiments simultaneously. The downregulation efficiency of *Djck1 $\alpha$*  and *Djslit* in single and double RNAi animals was demonstrated by qRT-PCR (Figure S3). *Djslit* RNAi animals all exhibited a single eye in the newly regenerated head as previously reported (8/8) (Figure 4E) [47]. Interestingly, *Djck1 $\alpha$*  and *Djslit* double RNAi animals (13/22) showed two normal eyes, while the remaining 9/22 *slit/ck1 $\alpha$*  RNAi animals showed one central eye (Figure 4E). These data demonstrate that *ck1 $\alpha$*  has a restriction on the expansion of the medial tissues by restricting the expression of *slit* in planarians. Then, we performed qRT-PCR to investigate the expression of other PCGs as *wnt5*, *wnt1*, *bmp4* and  $\beta$ -*catenin* after *ck1 $\alpha$*  RNAi (Figure S4). We found that with the downregulation of the endogenous *ck1 $\alpha$* , the *slit* gene showed higher expression, and the *wnt1* and *wnt5* genes showed no significant changes, while the expression levels of  $\beta$ -*catenin* and *bmp4* decreased at 8 days post RNAi. We next performed double RNAis with  $\beta$ -*catenin* and *bmp4*, which correspond to AP polarity and DV polarity, respectively (Figure S5). By day 14,  $\beta$ -*catenin* RNAi animals exhibited two heads (5/6), whereas *ck1 $\alpha$* & $\beta$ -*catenin* RNAi animals showed outgrowths on both heads (3/6) (Figure S5A), suggesting that the extra outgrowth caused by *Djck1 $\alpha$*  RNAi at the midline is independent of AP polarity. The *ck1 $\alpha$* &*bmp4* RNAi animals showed a more obvious bulge and a thicker body than *bmp4* RNAi or *ck1 $\alpha$*  RNAi (Figure S5B), suggesting that *ck1 $\alpha$*  RNAi enhances the defects related to DV patterning.

#### 4. Discussion

Casein kinase 1 $\alpha$  (CK1 $\alpha$ ), a conserved protein that exists and functions in a variety of signaling pathways, has been identified as a therapeutic target in some cancers [68,69]. In *zebrafish*, the expression pattern of *ck1 $\alpha$*  is ubiquitously expressed in early stages of the development. At 24 and 48 hpf, cross and longitudinal sections of the embryo show that *ck1 $\alpha$*  expression is not uniform and seems to be concentrated in some cell clusters in the brain and neural tube [70]. In *C. elegans*, KIN-19/CK1 $\alpha$  has been shown to regulate seam stem cell asymmetric division via a Wnt/ $\beta$ -catenin pathway, as well as seam stem cell terminal differentiation in tandem with the heterochronic/temporal identity pathway [21]. Meanwhile, previous studies have suggested that CK1 $\alpha$  has a significant effect on axis polarity. However, in the fields of regeneration, little is known about the role of CK1 $\alpha$ .

Planarians have constituted an excellent model in which to study polarity specification. The WNT/ $\beta$ -catenin signaling pathway has been shown to participate in tissue regeneration and polarity re-establishment.  $\beta$ -catenin functions as a molecular switch to decide and maintain anteroposterior identity in the planarian *Schmidtea mediterranea* [40]. Recently, the NR4A or SRC was proved to act on WNT signaling to pattern the planarian anterior–posterior axis [71,72]. The BMP pathway is essential for re-specification and maintenance of the dorsal–ventral (DV) axis. The SLIT protein has been emphasized to regulate the planarian midline in medial–lateral (ML) axis [47,73].

Herein we identified a *ck1 $\alpha$*  gene from the planarian *Dugesia japonica* based on the similarity of its predicted product to CK1 $\alpha$  proteins from other organisms. RNAi silencing of CK1 $\alpha$  resulted in defects in the medial tissues including the brain, ventral nerve cord cells bodies, dorsal epidermis and intestinal tissues, suggesting that CK1 $\alpha$  is required for organizing the mediolateral axis (Figures 2A–C and 4A–D). We propose that

the defects are a kind of expansion of the medial tissues, for we also detected hyper-proliferation and observed an outgrowth on the dorsal in the middle of the planarian body (Figures 1C,D and 3B,C). Recent studies have implicated that CK1 $\alpha$  can enhance the Wnt signaling by interacting with PAWS1 (protein associated with Smad1), a regulator of SMAD1 in BMP signaling that has been shown to induce the formation of a secondary axis in *Xenopus* embryos. These findings indirectly or directly suggest that CK1 $\alpha$  plays an important role in polarity establishment during development [22]. Consistent with this, our results suggest that CK1 $\alpha$  limits the mediolateral axis into a suitable range, which provides new insights into CK1 $\alpha$  in the study of axis polarity in planarians.

Planarian regeneration is guided by molecular mechanisms that restore the identity of the tissue. The mechanisms that control the expression of pole-specific gene programs remain elusive, despite emerging data regarding the expression of signaling molecules for polarity initiation. Abnormalities of the medial tissue defects including the intestine and nervous system resulting from *ck1 $\alpha$*  RNAi showed similarities with the consequences of *slit* RNAi (Figure 4A–C). However, the CNS, which was collapsed in *slit* RNAi animals, is labeled with more intensity by *ck1 $\alpha$*  RNAi (Figure 4A), indicating that *ck1 $\alpha$*  may function as a negative regulator of *slit*. Indeed, an increase in *slit* expressing cells was induced by *ck1 $\alpha$*  RNAi (Figure 4D). *Djck1 $\alpha$*  and *Djslit* double RNAi can rescue the less eye phenotype caused by *Djslit* RNAi (Figure 4E). Furthermore, the double RNAi phenomena of *ck1 $\alpha$* & $\beta$ -*catenin* or *ck1 $\alpha$* &*bmp4* show that the *Djck1 $\alpha$*  RNAi can cause extra outgrowth when DV (*bmp4* RNAi) polarity is disturbed, suggesting that *ck1 $\alpha$*  RNAi can enhance the defects related to DV patterning. Meanwhile, the CK1 $\alpha$  protein was previously reported to interact with PAWS1, and this kind of interaction is essential for PAWS1-dependent axis duplication, which suggests that CK1 $\alpha$  may be involved in BMP signaling in this manner as well. Therefore, these findings further suggest *ck1 $\alpha$*  is required for medial tissues regenerating and maintenance in planarians mainly by regulating BMP signaling. However, the mechanisms by which *ck1 $\alpha$*  and *slit* regulate the mediolateral axis and coordinately organize it remains to be determined.

**Supplementary Materials:** The following supporting information can be downloaded at: <https://www.mdpi.com/article/10.3390/cells12030473/s1>, Figure S1: Multiple sequence alignment of *Djck1 $\alpha$*  from *Dugesia japonica*, Homo sapiens, Mus musculus, Drosophila serrata, Xenopus laevis, and Danio rerio; Figure S2: The WISH with *Djmhca* probes in *Djck1 $\alpha$*  RNAi animals; Figure S3: The downregulation efficiency of *Djck1 $\alpha$*  and *Djslit* in single and double RNAi animals; Figure S4: Related gene expression after *ck1 $\alpha$*  RNAi; Figure S5: Regeneration defects induced by the double RNAi; Table S1: PCR primers used in this study.

**Author Contributions:** Y.H. performed the experiments, analyzed the data and wrote this manuscript. Y.S., Y.G. and M.M. performed experiments and analyzed the data. Q.T. and S.Z. designed the experiments, interpreted the data, and revised the manuscript with respect to intellectual content. All authors have read and agreed to the published version of the manuscript.

**Funding:** This research was funded by National Natural Science Foundation of China (31970419), Bingtuan Science and Technology Project (2019AB034) and Scientific and technological innovation talents in Colleges of Henan (21HASTIT034).

**Institutional Review Board Statement:** Not applicable.

**Informed Consent Statement:** Not applicable.

**Data Availability Statement:** Not applicable.

**Conflicts of Interest:** The authors declare no conflict of interest.

## References

1. Lemeer, S.; Heck, A.J. The phosphoproteomics data explosion. *Curr. Opin. Chem. Biol.* **2009**, *13*, 414–420. [[CrossRef](#)] [[PubMed](#)]
2. Sikes, R.A. Chemistry and pharmacology of anticancer drugs. *Br. J. Cancer* **2007**, *97*, 1713. [[CrossRef](#)]
3. Cheong, J.K.; Virshup, D.M. Casein kinase 1: Complexity in the family. *Int. J. Biochem. Cell. Biol.* **2011**, *43*, 465–469. [[CrossRef](#)]

4. Gross, S.D.; Anderson, R.A. Casein kinase I: Spatial organization and positioning of a multifunctional protein kinase family. *Cell Signal* **1998**, *10*, 699–711. [[CrossRef](#)] [[PubMed](#)]
5. DeMaggio, A.J.; Lindberg, R.A.; Hunter, T.; Hoekstra, M.F. The budding yeast HRR25 gene product is a casein kinase I isoform. *Proc. Natl. Acad. Sci. USA* **1992**, *89*, 7008–7012. [[CrossRef](#)]
6. Dhillon, N.; Hoekstra, M.F. Characterization of two protein kinases from *Schizosaccharomyces pombe* involved in the regulation of DNA repair. *EMBO J.* **1994**, *13*, 2777–2788. [[CrossRef](#)]
7. Robinson, L.C.; Hubbard, E.J.; Graves, P.R.; DePaoli-Roach, A.A.; Roach, P.J.; Kung, C.; Haas, D.W.; Hagedorn, C.H.; Goebel, M.; Culbertson, M.R.; et al. Yeast casein kinase I homologues: An essential gene pair. *Proc. Natl. Acad. Sci. USA* **1992**, *89*, 28–32. [[CrossRef](#)]
8. Chen, Y.; Jiang, J. Decoding the phosphorylation code in Hedgehog signal transduction. *Cell Res.* **2013**, *23*, 186–200. [[CrossRef](#)]
9. MacDonald, B.T.; Tamai, K.; He, X. Wnt/beta-catenin signaling: Components, mechanisms, and diseases. *Dev. Cell* **2009**, *17*, 9–26. [[CrossRef](#)]
10. Knippschild, U.; Gocht, A.; Wolff, S.; Huber, N.; Lohler, J.; Stoter, M. The casein kinase 1 family: Participation in multiple cellular processes in eukaryotes. *Cell Signal* **2005**, *17*, 675–689. [[CrossRef](#)]
11. Walczak, C.E.; Anderson, R.A.; Nelson, D.L. Identification of a family of casein kinases in *Paramecium*: Biochemical characterization and cellular localization. *Biochem. J.* **1993**, *296 Pt 3*, 729–735. [[CrossRef](#)] [[PubMed](#)]
12. Kearney, P.H.; Ebert, M.; Kuret, J. Molecular cloning and sequence analysis of two novel fission yeast casein kinase-1 isoforms. *Biochem. Biophys. Res. Commun.* **1994**, *203*, 231–236. [[CrossRef](#)] [[PubMed](#)]
13. Wang, P.C.; Vancura, A.; Mitcheson, T.G.; Kuret, J. Two genes in *Saccharomyces cerevisiae* encode a membrane-bound form of casein kinase-1. *Mol. Biol. Cell* **1992**, *3*, 275–286. [[CrossRef](#)] [[PubMed](#)]
14. Plowman, G.D.; Sudarsanam, S.; Bingham, J.; Whyte, D.; Hunter, T. The protein kinases of *Caenorhabditis elegans*: A model for signal transduction in multicellular organisms. *Proc. Natl. Acad. Sci. USA* **1999**, *96*, 13603–13610. [[CrossRef](#)] [[PubMed](#)]
15. Zhang, L.; Jia, J.; Wang, B.; Amanai, K.; Wharton, K.A., Jr.; Jiang, J. Regulation of wingless signaling by the CKI family in *Drosophila* limb development. *Dev. Biol.* **2006**, *299*, 221–237. [[CrossRef](#)] [[PubMed](#)]
16. Morrison, D.K.; Murakami, M.S.; Cleghon, V. Protein kinases and phosphatases in the *Drosophila* genome. *J. Cell Biol.* **2000**, *150*, F57–F62. [[CrossRef](#)] [[PubMed](#)]
17. Hanks, S.K.; Hunter, T. Protein kinases 6. The eukaryotic protein kinase superfamily: Kinase (catalytic) domain structure and classification. *FASEB J.* **1995**, *9*, 576–596. [[CrossRef](#)] [[PubMed](#)]
18. Graves, P.R.; Haas, D.W.; Hagedorn, C.H.; DePaoli-Roach, A.A.; Roach, P.J. Molecular cloning, expression, and characterization of a 49-kilodalton casein kinase I isoform from rat testis. *J. Biol. Chem.* **1993**, *268*, 6394–6401. [[CrossRef](#)] [[PubMed](#)]
19. Lubben, T.H.; Traugh, J.A. Cyclic nucleotide-independent protein kinases from rabbit reticulocytes. Purification and characterization of protease-activated kinase II. *J. Biol. Chem.* **1983**, *258*, 13992–13997. [[CrossRef](#)] [[PubMed](#)]
20. Peters, J.M.; McKay, R.M.; McKay, J.P.; Graff, J.M. Casein kinase I transduces Wnt signals. *Nature* **1999**, *401*, 345–350. [[CrossRef](#)] [[PubMed](#)]
21. Banerjee, D.; Chen, X.; Lin, S.Y.; Slack, F.J. kin-19/casein kinase Ialpha has dual functions in regulating asymmetric division and terminal differentiation in *C. elegans* epidermal stem cells. *Cell Cycle* **2010**, *9*, 4748–4765. [[CrossRef](#)] [[PubMed](#)]
22. Bozatz, P.; Dingwell, K.S.; Wu, K.Z.; Cooper, F.; Cummins, T.D.; Hutchinson, L.D.; Vogt, J.; Wood, N.T.; Macartney, T.J.; Varghese, J.; et al. PAWS1 controls Wnt signalling through association with casein kinase Ialpha. *EMBO Rep.* **2018**, *19*, e44807. [[CrossRef](#)] [[PubMed](#)]
23. Wagner, D.E.; Wang, I.E.; Reddien, P.W. Clonogenic neoblasts are pluripotent adult stem cells that underlie planarian regeneration. *Science* **2011**, *332*, 811–816. [[CrossRef](#)] [[PubMed](#)]
24. Zeng, A.; Li, H.; Guo, L.; Gao, X.; McKinney, S.; Wang, Y.; Yu, Z.; Park, J.; Semerad, C.; Ross, E.; et al. Prospectively Isolated Tetraspanin(+) Neoblasts Are Adult Pluripotent Stem Cells Underlying Planaria Regeneration. *Cell* **2018**, *173*, 1593–1608 e1520. [[CrossRef](#)] [[PubMed](#)]
25. Reddien, P.W.; Sanchez Alvarado, A. Fundamentals of planarian regeneration. *Annu. Rev. Cell Dev. Biol.* **2004**, *20*, 725–757. [[CrossRef](#)] [[PubMed](#)]
26. Salo, E. The power of regeneration and the stem-cell kingdom: Freshwater planarians (Platyhelminthes). *Bioessays* **2006**, *28*, 546–559. [[CrossRef](#)]
27. Hyman, L.H. The Invertebrates: Platyhelminthes and Rhynchocoela: The Acoelomate Bilateria. *Q. Rev. Biol.* **1951**, *2*, 550.
28. Reddien, P.W. The Cellular and Molecular Basis for Planarian Regeneration. *Cell* **2018**, *175*, 327–345. [[CrossRef](#)]
29. Newmark, P.A.; Sanchez Alvarado, A. Not your father's planarian: A classic model enters the era of functional genomics. *Nat. Rev. Genet.* **2002**, *3*, 210–219. [[CrossRef](#)]
30. Agata, K. Regeneration and gene regulation in planarians. *Curr. Opin. Genet. Dev.* **2003**, *13*, 492–496. [[CrossRef](#)]
31. Sánchez Alvarado, A. Planarian Regeneration: Its End Is Its Beginning. *Cell* **2006**, *124*, 241–245. [[CrossRef](#)] [[PubMed](#)]
32. Reddien, P.W.; Oviedo, N.J.; Jennings, J.R.; Jenkin, J.C.; Sánchez Alvarado, A. SMEDWI-2 is a PIWI-like protein that regulates planarian stem cells. *Science* **2005**, *310*, 1327–1330. [[CrossRef](#)] [[PubMed](#)]
33. Lapan, S.W.; Reddien, P.W. dlx and sp6-9 Control optic cup regeneration in a prototypic eye. *PLoS Genet.* **2011**, *7*, e1002226. [[CrossRef](#)] [[PubMed](#)]

34. Witchley, J.N.; Mayer, M.; Wagner, D.E.; Owen, J.H.; Reddien, P.W. Muscle cells provide instructions for planarian regeneration. *Cell Rep.* **2013**, *4*, 633–641. [[CrossRef](#)]
35. Scimone, M.L.; Cote, L.E.; Rogers, T.; Reddien, P.W. Two FGFR-L-Wnt circuits organize the planarian anteroposterior axis. *Elife* **2016**, *5*, e12845. [[CrossRef](#)]
36. Fincher, C.T.; Wurtzel, O.; de Hoog, T.; Kravarik, K.M.; Reddien, P.W. Cell type transcriptome atlas for the planarian *Schmidtea mediterranea*. *Science* **2018**, *360*, eaaq1736. [[CrossRef](#)]
37. Reddien, P.W. Constitutive gene expression and the specification of tissue identity in adult planarian biology. *Trends Genet.* **2011**, *27*, 277–285. [[CrossRef](#)]
38. Umesonu, Y.; Tasaki, J.; Nishimura, Y.; Hroudá, M.; Kawaguchi, E.; Yazawa, S.; Nishimura, O.; Hosoda, K.; Inoue, T.; Agata, K. The molecular logic for planarian regeneration along the anterior-posterior axis. *Nature* **2013**, *500*, 73–76. [[CrossRef](#)]
39. Yazawa, S.; Umesonu, Y.; Hayashi, T.; Tarui, H.; Agata, K. Planarian Hedgehog/Patched establishes anterior-posterior polarity by regulating Wnt signaling. *Proc. Natl. Acad. Sci. USA* **2009**, *106*, 22329–22334. [[CrossRef](#)]
40. Gurley, K.A.; Rink, J.C.; Sanchez Alvarado, A. Beta-catenin defines head versus tail identity during planarian regeneration and homeostasis. *Science* **2008**, *319*, 323–327. [[CrossRef](#)]
41. Petersen, C.P.; Reddien, P.W. Smed-betacatenin-1 is required for anteroposterior blastema polarity in planarian regeneration. *Science* **2008**, *319*, 327–330. [[CrossRef](#)] [[PubMed](#)]
42. Kobayashi, C.; Saito, Y.; Ogawa, K.; Agata, K. Wnt signaling is required for antero-posterior patterning of the planarian brain. *Dev. Biol.* **2007**, *306*, 714–724. [[CrossRef](#)] [[PubMed](#)]
43. Adell, T.; Salo, E.; Boutros, M.; Bartscherer, K. Smed-Evi/Wntless is required for beta-catenin-dependent and -independent processes during planarian regeneration. *Development* **2009**, *136*, 905–910. [[CrossRef](#)]
44. Gurley, K.A.; Elliott, S.A.; Simakov, O.; Schmidt, H.A.; Holstein, T.W.; Sanchez Alvarado, A. Expression of secreted Wnt pathway components reveals unexpected complexity of the planarian amputation response. *Dev. Biol.* **2010**, *347*, 24–39. [[CrossRef](#)] [[PubMed](#)]
45. Molina, M.D.; Salo, E.; Cebria, F. The BMP pathway is essential for re-specification and maintenance of the dorsoventral axis in regenerating and intact planarians. *Dev. Biol.* **2007**, *311*, 79–94. [[CrossRef](#)] [[PubMed](#)]
46. Gavino, M.A.; Reddien, P.W. A Bmp/Admp regulatory circuit controls maintenance and regeneration of dorsal-ventral polarity in planarians. *Curr. Biol.* **2011**, *21*, 294–299. [[CrossRef](#)]
47. Cebria, F.; Guo, T.; Jopek, J.; Newmark, P.A. Regeneration and maintenance of the planarian midline is regulated by a slit orthologue. *Dev. Biol.* **2007**, *307*, 394–406. [[CrossRef](#)]
48. Tian, Q.N.; Bao, Z.X.; Lu, P.; Qin, Y.F.; Chen, S.J.; Liang, F.; Mai, J.; Zhao, J.M.; Zhu, Z.Y.; Zhang, Y.Z.; et al. Differential expression of microRNA patterns in planarian normal and regenerative tissues. *Mol. Biol. Rep.* **2012**, *39*, 2653–2658. [[CrossRef](#)]
49. Tian, Q.; Sun, Y.; Gao, T.; Li, J.; Fang, H.; Zhang, S. Djnedd4L Is Required for Head Regeneration by Regulating Stem Cell Maintenance in Planarians. *Int. J. Mol. Sci.* **2021**, *22*, 11707. [[CrossRef](#)]
50. Tian, Q.; Guo, Q.; Guo, Y.; Luo, L.; Kristiansen, K.; Han, Z.; Fang, H.; Zhang, S. Whole-genome sequence of the planarian *Dugesia japonica* combining Illumina and PacBio data. *Genomics* **2022**, *114*, 110293. [[CrossRef](#)]
51. Rouhana, L.; Weiss, J.A.; Forsthoefel, D.J.; Lee, H.; King, R.S.; Inoue, T.; Shibata, N.; Agata, K.; Newmark, P.A. RNA interference by feeding in vitro-synthesized double-stranded RNA to planarians: Methodology and dynamics. *Dev. Dyn.* **2013**, *242*, 718–730. [[CrossRef](#)]
52. Cebria, F.; Newmark, P.A. Planarian homologs of netrin and netrin receptor are required for proper regeneration of the central nervous system and the maintenance of nervous system architecture. *Development* **2005**, *132*, 3691–3703. [[CrossRef](#)] [[PubMed](#)]
53. Guo, Q.; Zhao, G.; Ni, J.; Guo, Y.; Zhang, Y.; Tian, Q.; Zhang, S. Down-regulate of Djrfc2 causes tissues hypertrophy during planarian regeneration. *Biochem. Biophys. Res. Commun.* **2017**, *493*, 1224–1229. [[CrossRef](#)] [[PubMed](#)]
54. Ma, K.; Zhang, Y.; Song, G.; Wu, M.; Chen, G. Identification of Autophagy-Related Gene 7 and Autophagic Cell Death in the Planarian *Dugesia japonica*. *Front. Physiol.* **2018**, *9*, 1223. [[CrossRef](#)] [[PubMed](#)]
55. Livak, K.J.; Schmittgen, T.D. Analysis of relative gene expression data using real-time quantitative PCR and the 2(-Delta Delta C(T)) Method. *Methods (San Diego Calif.)* **2001**, *25*, 402–408. [[CrossRef](#)] [[PubMed](#)]
56. Collins, J.J., 3rd; Hou, X.; Romanova, E.V.; Lambrus, B.G.; Miller, C.M.; Saberi, A.; Sweedler, J.V.; Newmark, P.A. Genome-wide analyses reveal a role for peptide hormones in planarian germline development. *PLoS Biol.* **2010**, *8*, e1000509. [[CrossRef](#)] [[PubMed](#)]
57. Cebria, F.; Kobayashi, C.; Umesonu, Y.; Nakazawa, M.; Mineta, K.; Ikeo, K.; Gojobori, T.; Itoh, M.; Taira, M.; Sanchez Alvarado, A.; et al. FGFR-related gene nou-darake restricts brain tissues to the head region of planarians. *Nature* **2002**, *419*, 620–624. [[CrossRef](#)]
58. Cebria, F.; Newmark, P.A. Morphogenesis defects are associated with abnormal nervous system regeneration following roboA RNAi in planarians. *Development* **2007**, *134*, 833–837. [[CrossRef](#)]
59. Pearson, B.J.; Sánchez Alvarado, A. A planarian p53 homolog regulates proliferation and self-renewal in adult stem cell lineages. *Development* **2010**, *137*, 213–221. [[CrossRef](#)]
60. Tazaki, A.; Kato, K.; Orii, H.; Agata, K.; Watanabe, K. The body margin of the planarian *Dugesia japonica*: Characterization by the expression of an intermediate filament gene. *Dev. Genes Evol.* **2002**, *212*, 365–373. [[CrossRef](#)]
61. Tu, K.C.; Cheng, L.C.; TK Vu, H.; Lange, J.J.; McKinney, S.A.; Seidel, C.W.; Sanchez Alvarado, A. Egr-5 is a post-mitotic regulator of planarian epidermal differentiation. *Elife* **2015**, *4*, e10501. [[CrossRef](#)]

62. Tian, Q.; Zhao, G.; Sun, Y.; Yuan, D.; Guo, Q.; Zhang, Y.; Liu, J.; Zhang, S. Exportin-1 is required for the maintenance of the planarian epidermal lineage. *Int. J. Biol. Macromol.* **2019**, *126*, 1050–1055. [[CrossRef](#)] [[PubMed](#)]
63. Wurtzel, O.; Oderberg, I.M.; Reddien, P.W. Planarian Epidermal Stem Cells Respond to Positional Cues to Promote Cell-Type Diversity. *Dev. Cell* **2017**, *40*, 491–504.e495. [[CrossRef](#)]
64. Sakai, T.; Kato, K.; Watanabe, K.; Orii, H. Planarian pharynx regeneration revealed by the expression of myosin heavy chain-A. *Int. J. Dev. Biol.* **2002**, *46*, 329–332. [[PubMed](#)]
65. Fuchs, E.; Chen, T. A matter of life and death: Self-renewal in stem cells. *EMBO Rep.* **2013**, *14*, 39–48. [[CrossRef](#)] [[PubMed](#)]
66. Lin, A.Y.T.; Pearson, B.J. Yorkie is required to restrict the injury responses in planarians. *PLoS Genet.* **2017**, *13*, e1006874. [[CrossRef](#)]
67. Rossi, L.; Salvetti, A.; Lena, A.; Batistoni, R.; Deri, P.; Pugliesi, C.; Loreti, E.; Gremigni, V. DjPiwi-1, a member of the PAZ-Piwi gene family, defines a subpopulation of planarian stem cells. *Dev. Genes Evol.* **2006**, *216*, 335–346. [[CrossRef](#)]
68. Jiang, J. CK1 in Developmental Signaling: Hedgehog and Wnt. *Curr. Top. Dev. Biol.* **2017**, *123*, 303–329. [[CrossRef](#)]
69. Janovska, P.; Normant, E.; Miskin, H.; Bryja, V. Targeting Casein Kinase 1 (CK1) in Hematological Cancers. *Int. J. Mol. Sci.* **2020**, *21*, 9026. [[CrossRef](#)]
70. Albornoz, A.; Yáñez, J.M.; Foerster, C.; Aguirre, C.; Pereiro, L.; Burzio, V.; Moraga, M.; Reyes, A.E.; Antonelli, M. The CK1 gene family: Expression patterning in zebrafish development. *Biol. Res.* **2007**, *40*, 251–266. [[CrossRef](#)]
71. Li, D.J.; McMann, C.L.; Reddien, P.W. Nuclear receptor NR4A is required for patterning at the ends of the planarian anterior-posterior axis. *Elife* **2019**, *8*, e42015. [[CrossRef](#)] [[PubMed](#)]
72. Bonar, N.A.; Gittin, D.I.; Petersen, C.P. Src acts with WNT/FGFRL signaling to pattern the planarian anteroposterior axis. *Development* **2022**, *149*, dev200125. [[CrossRef](#)] [[PubMed](#)]
73. Molina, M.D.; Neto, A.; Maeso, I.; Gomez-Skarmeta, J.L.; Salo, E.; Cebria, F. Noggin and noggin-like genes control dorsoventral axis regeneration in planarians. *Curr. Biol.* **2011**, *21*, 300–305. [[CrossRef](#)] [[PubMed](#)]

**Disclaimer/Publisher's Note:** The statements, opinions and data contained in all publications are solely those of the individual author(s) and contributor(s) and not of MDPI and/or the editor(s). MDPI and/or the editor(s) disclaim responsibility for any injury to people or property resulting from any ideas, methods, instructions or products referred to in the content.